
Faculty of Engineering

Faculty Publications

Natural Biomaterials and Their Use as Bioinks for Printing Tissues

Claire Benwood, Josie Chrenek, Rebecca L. Kirsch, Nadia Z. Masri, Hannah Richards, Kyra Teetzen, & Stephanie M. Willerth

February 2021

© 2021 Claire Benwood et al. This is an open access article distributed under the terms of the Creative Commons Attribution License. <https://creativecommons.org/licenses/by/4.0/>

This article was originally published at:

<https://doi.org/10.3390/bioengineering8020027>

Citation for this paper:

Benwood, C., Chrenek, J., Kirsch, R. L., Masri, N. Z., Richards, H., Teetzen, K., & Willerth, S. M. (2021). Natural Biomaterials and Their Use as Bioinks for Printing Tissues. *Bioengineering*, 8(2), 1-19. <https://doi.org/10.3390/bioengineering8020027>.

Review

Natural Biomaterials and Their Use as Bioinks for Printing Tissues

Claire Benwood ^{1,†}, Josie Chrenek ^{2,†} , Rebecca L. Kirsch ^{3,†}, Nadia Z. Masri ^{4,†}, Hannah Richards ^{2,†}, Kyra Teetzen ^{2,†} and Stephanie M. Willerth ^{1,2,4,*} 

¹ Department of Mechanical Engineering, University of Victoria, Victoria, BC V8P 5C2, Canada; cbenwood@uvic.ca

² Biomedical Engineering Program, University of Victoria, Victoria, BC V8P 5C2, Canada; josiec@live.ca (J.C.); hannahrichards@uvic.ca (H.R.); kyrateetzen3@gmail.com (K.T.)

³ Department of Chemistry, University of Victoria, Victoria, BC V8P 5C2, Canada; rebeccakirsch@uvic.ca

⁴ Division of Medical Sciences, University of Victoria, Victoria, BC V8P 5C2, Canada; nadiam@uvic.ca

* Correspondence: willerth@uvic.ca; Tel.: +1-(250)-721-7303

† These authors contributed equally to this work.

Abstract: The most prevalent form of bioprinting—extrusion bioprinting—can generate structures from a diverse range of materials and viscosities. It can create personalized tissues that aid in drug testing and cancer research when used in combination with natural bioinks. This paper reviews natural bioinks and their properties and functions in hard and soft tissue engineering applications. It discusses agarose, alginate, cellulose, chitosan, collagen, decellularized extracellular matrix, dextran, fibrin, gelatin, gellan gum, hyaluronic acid, Matrigel, and silk. Multi-component bioinks are considered as a way to address the shortfalls of individual biomaterials. The mechanical, rheological, and cross-linking properties along with the cytocompatibility, cell viability, and printability of the bioinks are detailed as well. Future avenues for research into natural bioinks are then presented.

Keywords: bioink; 3D bioprinting; biomaterials; tissue engineering; regenerative medicine



Citation: Benwood, C.; Chrenek, J.; Kirsch, R.L.; Masri, N.Z.; Richards, H.; Teetzen, K.; Willerth, S.M. Natural Biomaterials and Their Use as Bioinks for Printing Tissues. *Bioengineering* **2021**, *8*, 27. <https://doi.org/10.3390/bioengineering8020027>

Academic Editor: Houman Savoji

Received: 30 January 2021

Accepted: 17 February 2021

Published: 20 February 2021

Publisher's Note: MDPI stays neutral with regard to jurisdictional claims in published maps and institutional affiliations.



Copyright: © 2021 by the authors. Licensee MDPI, Basel, Switzerland. This article is an open access article distributed under the terms and conditions of the Creative Commons Attribution (CC BY) license (<https://creativecommons.org/licenses/by/4.0/>).

1. Introduction

3D bioprinting uses additive manufacturing (objects are made layer-by-layer) to create objects that mimic biological constructs by patterning living cells and other biological materials [1]. Bioinks are the materials used to contain cells when bioprinting tissues. They provide structure for the bioprinted tissue and support and nutrients for the cells, creating an environment in which the cells can survive, grow, and proliferate. Many materials and combinations of materials can be used as bioinks: hydrogels (water-based gels) are the most popular and promising because they are biocompatible and have similar properties to the extracellular matrix (ECM) [2–5]. The ECM is the non-cellular scaffold secreted by the cells of all tissues and organs [6,7]. It supports cells and provides biochemical and biomechanical cues for several biological processes, including cell proliferation and differentiation [6,7]. This paper reviews the properties and applications of several natural bioinks that are suitable for extrusion printing. Extrusion printing is the most commonly employed method of bioprinting as it can be used with a wide range of compatible materials and their associated viscosities Figure 1 [8–10].

Bioprinting technology allows for control over various properties of the engineered object, such as its shape, size, and internal porosity [11]. The main bioprinting methods are extrusion, inkjet, laser-assisted, and stereolithography [11–13]. The advantages associated with extrusion printing include the ability to: (i) print one construct with multiple printheads and materials; (ii) print constructs with differences throughout (different cell types, densities, and signaling molecules); and (iii) print with higher cell densities than other methods [9]. Limitations of this type of printing include high shear stress and pressure, which reduce cell viability and functionality [9]. Another printing method is inkjet

printing—a non-contact printing process (the printhead does not touch the object being printed) in which droplets of bioink are deposited onto a substrate or dish by a thermal actuator, piezoelectric actuator, or pressure-pulses [11,14]. Laser-assisted printing, based on the laser-induced forward transfer process, functions using energy from high-intensity lasers to deposit biomaterials [15]. Furthermore, stereolithography bioprinting uses digitally controlled light intensity to solidify a photo-sensitive material in a nozzle-free manner [16]. Many developed bioinks can be used for these printing methods, but a commonly cited challenge is creating suitable bioinks for different cells and applications since these often require specific bioink characteristics [17,18]. Additionally, these printing methods are similar to those used in other 3D printing applications for biomedical uses, including for 3D-printed prosthetics, customized surgical tools, and anatomical models [19–21]. However, these applications are beyond the scope of this review, which will focus on the use of bioprinting for tissue engineering purposes.

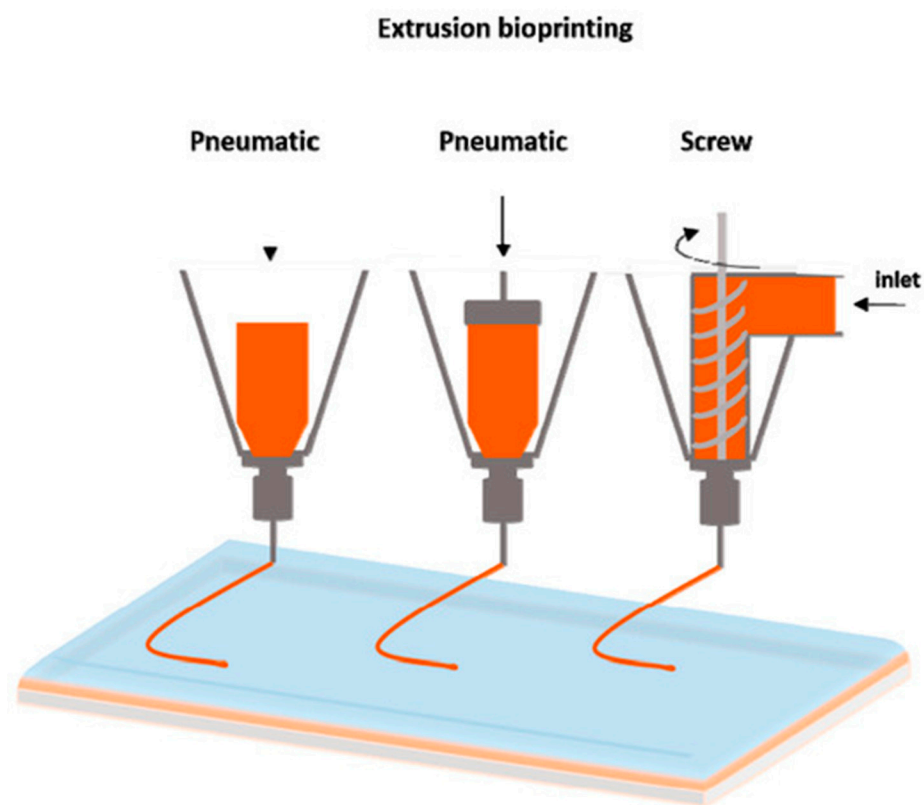


Figure 1. The main forms of extrusion printing [10]. This figure is being reprinted under a Creative Commons BY 4.0 license.

The 3D printing method dictates which properties the bioink must have before, during, and after gelation. Therefore, an effective bioink contains a combination of the following properties such as mechanical, including rheological, and crosslinking properties that are essential for shape fidelity and structural maintenance of the product, while cytocompatibility ensures the viability of the cells within the bioink [1,22]. The mechanical properties of a bioink can be tuned appropriately to ensure it meets strength requirements depending on the application. For example, load bearing organs like bone or cartilage will require a graft that demonstrates high mechanical strength [23]. Shear modulus and viscoelasticity are also important mechanical properties when considering various types of ECM [23]. For extrusion and droplet printing, shear thinning properties are required to compensate for the high shear stress developed during printing [24]. An important rheological property of bioinks is the viscosity; high viscosity allows the extruded filaments to maintain their shape before the crosslinking process that will set the print [25]. Additional factors to

consider when evaluating the printability of a bioink are physicochemical factors like the swelling properties and gelation kinetics, both of which are unique to the material [22]. The swelling behavior of the hydrogel will determine the final shape and size of the 3D printed structure and the gelation kinetics, which are related to the crosslinking method, help the construct maintain its structure [26]. For example, gelation can be either physical or chemical depending on the crosslinking method and the desired interactions within the hydrogel.

Bioink hydrogels may be composed of natural biomaterials, synthetic materials, or a combination that highlights the favorable properties of both components. Natural biomaterials offer a favorable environment for cell growth by mimicking the natural ECM of tissues, self-assembling, and exhibiting biocompatibility and biodegradation properties [24,27]. However, they lack the mechanical properties required to maintain structural integrity within the *in vivo* microenvironment and can be unpredictable and unstable [24,28]. Poor mechanical properties can lead to difficulties in printing, less rigid tissue structures, and decreased support for the cells in the tissue [24,27]. Synthetic materials are controllable and can have photocrosslinking ability; however, they can be more cytotoxic than natural materials and, therefore, the environment they create may not promote the survival of cells [1,24]. For instance, the use of synthetic crosslinking agents can cause cytotoxic effects on cells that can be lessened with natural crosslinkers [29].

Bioinks can be divided into two categories: scaffold-based and scaffold-free. Both bioink types can be utilized with extrusion printing. Scaffold-based bioinks incorporate cells into an exogenous biomaterial support structure Figure 2 [30–32]. This supporting scaffold is typically composed of hydrogels, microcarriers (porous, spherical structures to support cell growth and adhesion), or decellularized ECM (dECM) components [30]. The scaffold supports cell growth, proliferation, and differentiation while providing mechanical strength and biological and chemical cues to guide the assembly of a functional tissue [30,33]. Additionally, scaffolds are designed to degrade over time as the cells proliferate and begin to form the desired tissue. The scaffold is chosen in part based on its degradation rate, which should emulate the rate of ECM-formation by the cells incorporated into the construct [34]. Additionally, adjusting the rate of scaffold degradation can enable control over the release of growth and differentiation factors [34]. Although scaffold-based bioinks are designed to be highly biocompatible, challenges with these bioinks include host immunological responses during *in vivo* testing, material toxicity, disruption of cell-cell interactions, time requirements for scaffold degradation, and negative impacts of incompletely degraded scaffold on the mechanical properties of printed constructs [30,33,35–37].

In contrast, scaffold-free bioinks are composed solely of cells and their secreted matrices, without the need for supporting biomaterials [30,31,33]. These bioinks consist of cell aggregate structures, such as cell sheets, pellets, spheroids, or tissue strands, and rely on the ability of the cells to self-assemble into larger tissue constructs [30,31,34]. Scaffold-free bioinks eliminate the time requirements for scaffold degradation, reduce the need for extensive cell proliferation due to high initial seeding densities, minimize immunological responses *in vivo*, and improve cellular interactions and tissue biomimicry [33–35]. However, scaffold-based bioinks remain the most common due to their improved structural properties, reproducibility, scalability, and affordability [30,31,35]. Therefore, this review will focus on natural bioinks that belong to the scaffold-based category.

Natural bioinks have been applied to a diverse range of both soft and hard tissue engineering to create neural, cardiac, cartilage, vasculature, bone, and skin tissues [12,14,38–41]. Their ability to promote cell attachment and differentiation allow them to be used for drug testing and cancer research [42]. Personalized tissues can be created and, in the future, it may be possible to replicate whole organs for transplantation. The myriad combinations of the various bioinks described below allow for a wide range of functions.

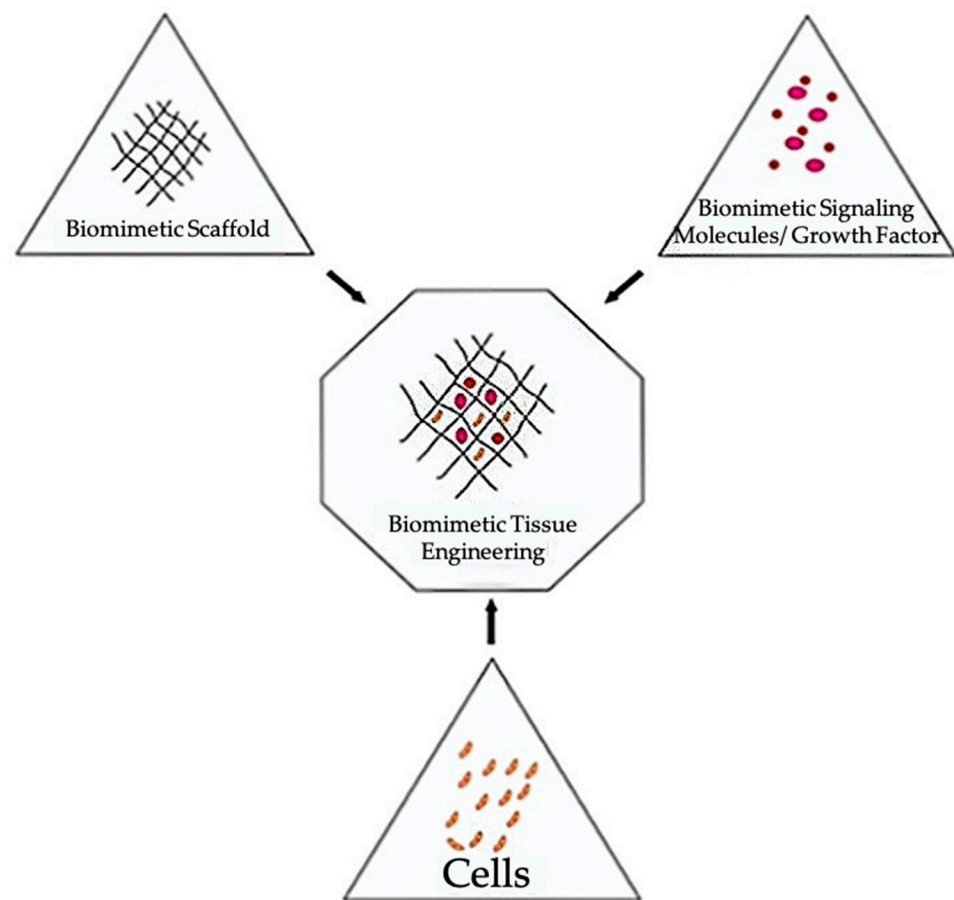


Figure 2. The main components used when constructing biomimetic tissues [32]. This figure is being reprinted under a Creative Commons BY 4.0 license.

2. Types of Natural Bioinks

A bioink should have and maintain similar properties to the targeted tissues, including: (i) physico-mechanical properties; and (ii) biological properties, to be considered biofunctional [24,43,44]. Not only does the bioink have to maintain cell viability, but it must also be printable. Accordingly, bioinks may be modified depending on the printer being used and the target tissue. For all these properties to be achieved, especially for extrusion-based bioprinting, a mix of two or more biomaterials is usually required [43,45]. Multicomponent bioinks are also often superior to those made up of solely one biomaterial as single component bioinks usually lack sufficient biocompatibility and high mechanical and functional requirements to form biomimicry tissues [45]. In addition, the components of multicomponent bioinks can complement one another, account for what the other bioink material might be lacking, and act as a supplementing element that can assist in the formation of more complex tissue constructs [43,45]. Furthermore, nanomaterials serve as an attractive addition to bioinks as they can lead to modifications, such as changes in bioink viscosity, and in some cases can make the bioink conductive, thus increasing signal transduction [44]. The following sections will discuss the properties of different natural bioinks, including agarose, alginate, gellan gum, dextran, hyaluronic acid (HA), silk, fibrin, collagen, dECM, Matrigel, cellulose, gelatin, and chitosan, and examples of common multicomponent bioinks and nanomaterials.

2.1. Agarose

Agarose is a natural polysaccharide derived from red seaweed that consists of repeating disaccharide units of D-galactose and 3,6-anhydro-L-galactopyranose [46,47]. Agarose is a part of the carbohydrate polymer family and is often used in tissue engineering appli-

cations due to its biocompatibility and thermo-reversible gelling mechanism [48]. When printed on its own, agarose is mainly used to help with mold formation when creating vascularized tissue constructs [33,46]. Norotte et al. used two printheads, with one dedicated to printing agarose rods to help control the wall thickness and diameter when creating tubular vascular grafts. The second printhead was used to deposit cell types, including fibroblasts and smooth muscle cells, into multicellular cylinders [33]. Agarose has also been used as part of a bioink designed to self-erode in order to form microchannels [49].

Agarose has a structure that resembles the ECM due to similar macromolecular properties [48]. Oxygen and other products can be diffused across its microstructure; therefore, it is often used as a component of bioinks to provide a support structure for cells [48]. Gu et al. created a bioink to print 3D neural mini-tissue constructs with agarose included in the ink specifically for structural support and to ensure the ideal viscosity of the bioink for printing [50]. Agarose hydrogels are also used to bioprint cartilage tissue [51]. Mesenchymal stem cell (MSC) laden agarose hydrogels were reinforced with 2% polycaprolactone (PCL) to increase stiffness [52]. This combination supports the production of hyaline cartilage and resulted in 80% cell viability after printing [52]. Native agarose does not react with other biological tissues and, therefore, it is often mixed with collagen, alginate, chitosan, or fibrin to increase its ability to support cell survival [47,48,53,54].

Carboxylated agarose is a derivative of native agarose with carboxylic acid groups on the polysaccharide backbone. Changing the degree of carboxylation causes an α -helix to β -sheet switch in secondary structure, allowing mechanical properties of the bioink to be modified without affecting the concentration [55,56]. Forget et al. bioprinted carboxylated agarose with human MSCs and achieved a 95% cell survival rate [57]. Gu et al. also created a carboxylated agarose-based bioink that had a high cell survival rate and was stiff enough to form 5–10 mm tall structures of various shapes without requiring extra support material [56]. Thus, agarose is a commonly used material for 3D printing applications.

2.2. Alginate

Alginate is a biocompatible anionic polymer derived from brown algae [58,59]. Alginates are block copolymers, and the exact sequence and ratio of α -L-guluronate and (1,4)-linked β -D-mannuronate residues depend on the alginate source [58,59]. Due to its biocompatibility and relatively low cost, alginate is commonly used for a variety of biomedical applications, including wound healing, drug delivery, and tissue engineering [58,59]. Alginate's main advantage as a bioink is its ability to form hydrogels with properties similar to those of tissues' ECM [58]. While mammals do not produce enzymes that cause alginate to degrade, other factors can impact its long-term stability in vivo. Alginate that is oxidized by periodate is prone to hydrolytic degradation, and ionically-crosslinked alginate gels erode in vivo due to divalent ions leaching into the media surrounding the gel [58,60]. Pure alginate also has low viscosity and zero shear viscosity, which impact its ability to retain its shape [61]. Alginate is unusual among natural bioinks in that it has very low bioactivity [61–63], which means that it does not support or promote cell proliferation. These barriers to using alginate as a bioink can be remedied by modifying it or mixing it with other materials. Adding nanocellulose has been shown to improve the rheological and mechanical properties and thus the printability of alginate-based bioinks [62]. Müller et al. added nanocellulose to alginate sulfate, which resulted in a bioink with improved rheological properties, a yield point instead of zero shear viscosity, and good day 28 cell viability [62]. Recently, Lee et al. found that adding methacrylated dECM to an alginate-based bioink improved the bioactivity [61]. Emami et al. explored oxidation as another method of stabilizing alginate bioinks [59]. Sodium periodate was used to oxidize sodium alginate, with different ratios of sodium alginate to sodium periodate resulting in different degrees of oxidation. Oxidizing the sodium alginate allowed its aldehyde groups to cross-link with the amine groups on gelatin, which resulted in a stable bioink with good cell adhesion, biocompatibility, and biodegradability properties [59]. Bioinks containing alginate have

applications in a variety of areas of tissue engineering, including the development of many types of bioprinted tissues, drug delivery, and wound treatment [58,59,61,62,64,65].

2.3. Cellulose

Cellulose serves as the primary structural material in plant cell walls due to its rigid structure [66]. It is a polysaccharide made up of (1–4) linked β -D-glucopyranosyl units [67]. Carboxymethyl cellulose (CMC), a cellulose ether that is water soluble, can be used to modify the viscosity of other polymers with less ideal rheologic properties [68]. In one study that created bone tissue constructs, CMC was combined with a poly(lactic-co-glycolic acid) bioink to create the ideal viscosity for deposition – the highest viscosity that would not obstruct the syringe tips. The addition of CMC also allowed for cells to be included in the ink and printed successfully [69]. Janarthanan et al. mixed CMC with glycol chitosan hydrogels to create a gel-based ink that had both stability and cell compatibility. The CMC provided reinforcement to the hydrogels, helping with the stability and shape fidelity of the final constructs [68,70].

Cellulose nanocrystals occur when the cellulose chains are highly ordered and can promote mechanical strength along with shear thinning behavior [71]. They are incorporated into many different bioinks, improving the elasticity, strength, and porosity of the constructs created, and when blended with other materials can also improve the viscosity of bioinks [72,73]. Jiang et al. created a bioink that incorporated cellulose nanocrystals into a bioink made of oxidized dextran and gelatin hydrogels. The CNC helped to improve the porosity of the constructs created [72]. Along with being biocompatible, nanocellulose does not enable bacterial growth, making it an attractive option for wound dressing applications [73]. Another study utilized the shear thinning of nanofibrillated cellulose and combined it with alginate in order to bioprint cartilage tissues. Human chondrocytes were successfully included in the ink and after 7 days had a cell viability of 86% [74]. These studies demonstrate the benefits of incorporating cellulose into a bioink blend.

2.4. Chitosan

Chitosan is a naturally derived polysaccharide that is made through chitin deacetylation. Chitosan is typically poorly soluble in water but can be dissolved in solutions with a pH of 6.2 or lower [75,76]. Furthermore, chitosan is nontoxic, biodegradable, biocompatible, bio-adhesive, and renewable [75,76]. However, chitosan has weak mechanical strength, which limits its use for creating hard tissues like cartilage [75].

He et al. modified chitosan with ethylenediaminetetraacetic acid (EDTA) before the addition of Ca^{2+} to increase the amount of chitosan- Ca^{2+} crosslinking, which enhanced the stability and mechanical properties of chitosan for chondrocyte support [75]. Varying concentrations of the two bioink components, chitosan and modified chitosan, resulted in altered printability and gelation abilities, and higher proportions of modified chitosan resulted in higher storage and loss moduli. Modified chitosan was the main component that contributed to strength enhancement. Furthermore, their bioink was analyzed and found to have low cytotoxicity, no effect of the hydrogel mesh on chondrocyte toxicity, no impedance on cell proliferation, fast gelation, high precision during printing, and the ability to tune mechanical strength and viscoelastic properties through the adjustment of the two component proportions [75]. In another study, a chitosan bioink was prepared by dissolving chitosan in an acidic mixture and its properties were analyzed for extrusion printing [76]. Concentrations of chitosan ink higher than 11 wt% and lower than 4 wt% were found to be too viscous and too dilute, respectively, while an optimal viscosity was found from a median concentration. The printed structures had high resolution (30 μm) and high shape retention. Good mechanical properties of the chitosan hydrogel (high max strength break of a neutralized filament was ~97 MPa in dry state, and high strain break at ~360% in a wet state) were found [76]. In conclusion, chitosan offers many advantages to bioprinting but often requires additional components to improve its mechanical strength.

2.5. Collagen

Collagens are the most prevalent proteins in mammals, comprising approximately 30% of the total mammalian protein mass [77]. They are hydrophilic proteins that are important structural components of the ECM [77,78]. Collagens consist of three polypeptide chains, known as α chains, and contain triple helical domains [77]. There are 28 different types of collagen, which are composed of varying quantities of triple helices and different combinations of α chains [77,78]. Collagens do not cause significant immunological responses and have integrin-binding domains, which promote cell adhesion, attachment, and growth [30]. However, the immunogenicity of collagen can be affected by the presence of other proteins, cell remnants, and crosslinking reagents, and animal-derived collagen may lead to inflammation and disease transmission [79,80]. Collagen type I is a member of the fibril-forming subfamily of collagens [78] and is commonly used in bioprinting [30]. However, it is not often used as a bioink on its own due to its mechanical instability and slow gelation rate at physiological temperatures, which limit its ability to hold its shape once extruded [30]. Collagen maintains a liquid state below 37 °C [30,81].

Studies using collagen alone as a bioink often aim to improve its mechanical properties by using sacrificial supports (temporary materials that maintain the structure of bioprinted constructs but are removed post-printing) [82,83] or by directly modifying characteristics of the collagen bioink, such as the concentration or crosslinking method utilized [84–86]. Several studies have also investigated methods to improve the printability of collagen by controlling the gelation kinetics and storage modulus of collagen bioinks [84,86,87]. An increased storage modulus, particularly one that significantly exceeds the loss modulus, has been found to correspond to improved printability of collagen [86]. Additionally, Diamantides et al. showed that both gelation kinetics and the storage modulus of collagen bioinks are dependent upon pH levels [84]. The average storage modulus after complete gelation was found to be highest at pH values of 7.5–8.0 and 8.0–8.5, but decreased outside of these ranges [84]. In this study, a blue light activated riboflavin crosslinker was also shown to increase the storage modulus of the collagen [84]. However, the riboflavin crosslinking resulted in an approximately 20% reduction in chondrocyte viability [84]. In a more recent study, it was found that the storage modulus of a type I collagen bioink was dependent on both the seeding density of cells and the degree of gelation [87]. Although the collagen maintained high levels of printability and chondrocyte viability across a range of cell densities, the storage modulus was found to increase with cell density before gelation but decreased with higher cell density after gelation [87].

Collagen is often combined with other biomaterials to improve the structural integrity, printability, and bioactive properties of natural bioinks. For instance, Yang et al. found that adding type I collagen to an alginate-based bioink improved its mechanical strength, helped preserve chondrocyte phenotypes, and suppressed undesired differentiation when printing cartilage constructs [51]. Similarly, the applicability of collagen-alginate composite bioinks for bioprinting of cartilage was demonstrated in a study by Liu et al., which showed that printed collagen-alginate hydrogels could support sustained drug release from incorporated PCL microspheres [88]. A recent study also examined the rheological properties of collagen-chitosan composite bioinks with different component ratios [89]. Collagen-chitosan blends exhibited shear-thinning behavior and negligible cytotoxicity effects on NIH-3T3 fibroblasts, which are encouraging properties for future work with this biomaterial combination [89]. Overall, extensive work has been done to optimize collagen as both a stand-alone bioink and as part of multicomponent bioinks.

2.6. Decellularized Extracellular Matrix

dECM is obtained through decellularization of tissues using a variety of physical and chemical methods, including freeze-thaw cycles, detergents, or enzymatic agents [90]. Although a certain amount of disruption to the ECM is unavoidable during this process, tissue decellularization aims to remove all cellular components of the tissue while maintaining as much of the structure and composition of the ECM as possible [90]. Retaining

the native structure of the ECM offers several benefits for use as a bioink material, including potential elimination of the need for crosslinker [91] and the ability to induce tissue-specific characteristics into printed constructs through choosing the tissue source of the dECM [7,91,92]. For instance, Han et al. tested four porcine-derived dECM bioinks from different sources (liver, heart, skin, and cornea) and demonstrated that the tissue source of the dECM generated tissue-specific gene expression in human bone marrow MSCs [92]. dECM is also one of the few natural biomaterials that is commonly used as a bioink on its own. dECM bioinks for extrusion printing have been produced using a variety of tissue sources, including the heart [91–96], skin [92,97–99], liver [92,100], intestines [101], cornea [92,102], bones [103], and tendons [104,105].

dECM has been significantly characterized for cardiac applications. Decellularized heart tissue has been shown to support the maturation, differentiation, and viability of cardiomyocytes [93,94]. Shin et al. demonstrated that incorporating Laponite-XLG nanoclay and poly(ethylene glycol) diacrylate (PEGDA) for photopolymerization could improve the structural fidelity of heart dECM bioinks laden with hiPSC-derived cardiomyocytes while maintaining over 94% viability after seven days [94]. Changing the concentration of PEGDA enabled tuning of the compressive Young's (or elastic) modulus, which can allow for better replication of the mechanical properties of both normal and fibrotic heart tissue [94]. Additionally, heart dECM bioinks have shown promise for printing human cardiac progenitor cells [95,96]. Jang et al. printed pre-vascularized stem cell patches composed of a heart dECM bioink laden with cardiac progenitor cells and MSCs [96]. In vivo testing in mice demonstrated that patches patterned with the two cell types promoted vascularization, maintained cell viability, and decreased cardiac remodeling and fibrosis [96].

Additionally, dECM bioinks have been validated for skin tissue engineering, particularly for wound healing applications. For instance, Kim et al. printed a pre-vascularized skin patch using skin-derived dECM laden with endothelial progenitor cells and adipose-derived stem cells, which promoted wound closure, epithelialization, neovascularization, and blood flow during in vivo testing in mice [97]. In vitro analysis also showed that the dECM constructs shrank less than collagen-based constructs [97]. Similarly, combining skin-derived dECM with a fibrinogen-based bioink was recently found to improve the mechanical properties and viability of a bioprinted skin model incorporated with primary human skin fibroblasts [98]. Collagen from the dECM improved the structural fidelity of the fibrinogen constructs and SEM imaging showed that the dECM and fibrinogen combination produced micro-architecture that resembled human skin [98]. These studies exemplify the beneficial properties of dECM bioinks for bioprinting a variety of tissues.

2.7. Dextran

Dextran is a natural, nontoxic, hydrophilic homopolysaccharide consisting mostly of α -1,6-linked D-glucopyranose residues [44,106]. Because dextran only contains hydroxyl groups, which do not provide support for cell attachment, it is common to chemically modify dextran to allow for functional affinity binding sites [106]. An advantage of dextran is that it can be used to create biodegradable scaffolds due to its degradation by dextranase, which is an enzyme naturally found in mammals [106].

Dextran is not typically used as a bioink by itself because of its poor mechanical strength, so it is often combined with other natural biomaterials [107]. Notably, oxidized dextran has been shown to act as a natural crosslinker for gelatin-based bioinks, resulting in improved printability and structural fidelity of extruded structures [72,108–110]. Pescosolido et al. utilized photocrosslinkable hydroxyethyl-methacrylate-derivatized dextran (dex-HEMA), a dextran derivative, to improve the stability of 3D-bioprinted HA hydrogels [111]. In this study, a semi-interpenetrating network scaffold of HA and dex-HEMA was printed and demonstrated high porosity, shear thinning at shear rates above 0.05 s^{-1} , and good structural integrity while maintaining the viability of encapsulated equine chondrocytes for three days [111]. Additionally, Harman et al. demonstrated that a

bioink composed of the synthetic polymer poly(ethylene-3,4-dioxythiophene) and dextran sulfate could be extrusion printed and could support the viability, morphology, and proliferation of fibroblasts when added to cell culture medium [112]. The conductive properties of this composite bioink could enable future applications involving the electrostimulation of cells [112].

2.8. Fibrin

Fibrinogen is a soluble protein found in blood and the enzyme thrombin catalyzes the digestion of fibrinogen into fibrin monomers. Fibrin is an insoluble, biocompatible, and biodegradable biopolymer with properties that can be adjusted by modifying the concentrations of both the thrombin and fibrinogen present [113]. Fibrin can also be blended with other materials such as PCL to adjust its properties [113]. This allows fibrin properties to imitate both hard and soft tissues. Fibrin is also a popular choice for bioinks because it allows for communication between cells due to its non-linear elasticity [113]. Fibrin-based bioinks are used to create a wide range of tissues including neural, cardiac, skin, and vascularized tissues [12,39,41,42,114]. Fibrin based bioink printed with Aspect Biosystems novel RX1 bioprinter showed cell viability levels of neural progenitor cells (NPCs) to be greater than 81% [115]. Sharma et al. combined this bioink with guggulsterone releasing microspheres in order to differentiate human induced pluripotent stem cell (hiPSC)-derived NPCs into neural tissues consisting of dopaminergic neurons [116]. Fibrin is a viscoelastic polymer that is often not printed as a stand-alone material due to its high viscosity that makes extrusion of the bioink challenging in its cross-linked form [117]. A lack of shear thinning behavior in fibrin does not allow for the decrease in viscosity required for the successful extrusion of bioink. Its pre-polymer form, fibrinogen, is also difficult to print alone because it is unable to maintain its shape [113].

These challenges in printing fibrin have been overcome by utilizing numerous different strategies, the first of which is crosslinking. Lee et al. created a tumor model to analyze a novel glioblastoma treatment. A fibrin-based bioink was printed with a crosslinker to polymerize the bioink as it was extruded from the microfluidic printhead [42]. Smits et al. utilized this same method and bioink to evaluate the effectiveness of Compound 15 in treating glioblastoma multiforme [118]. In a different study, both a bioink and crosslinker were extruded from two different needles to create a core-shell design [119]. The second strategy for printing fibrin is to use a support bath that helps to maintain the shape of the bioprinted construct [64]. Freeform reversible embedding of suspended hydrogels (FRESH)—a novel method of bioprinting used by Hinton et al.—was used to extrude a fibrinogen ink into a gelatin support bath containing thrombin that was then removed after printing to create bifurcated tubes [120]. Finally, the method of combining fibrinogen with materials that have more viscous properties, such as gelatin, was used to bioprint cardiomyocyte-laden constructs [121].

2.9. Gelatin

Gelatin, a natural polymer created through collagen hydrolysis, has been widely used as a bioink component [122]. Gelatin can form hydrogels after being cooled at low temperatures (20–30 °C) and is thermo-sensitive, meaning its bonds are easily broken by heat, resulting in its ability to be printed and stacked on itself in a controlled fashion [123]. Gelatin provides good biocompatibility, solubility, and degradability to bioinks [122]. As well, the viscosity of gelatin-based bioinks can be easily changed by altering the temperature or concentration of gelatin within the bioink. This is advantageous since certain viscosities are not compatible with extrusion bioprinting. Gelatin also has a number of side chains that allow for its chemical crosslinking and modification [122,124].

Gelatin has been combined with other natural or synthetic materials when manufacturing bioinks due to its many advantages [107,108,125]. For example, its quick gelation at moderate temperatures gives printed constructs strong initial stability even when printed with other, less stable materials [126]. Afterwards, when in physiological con-

ditions, the gelatin will dissolve, leaving the other biomaterial (e.g., silk) behind [126]. Unmodified gelatin does not crosslink alone and requires chemical reactions (e.g., with N,N-(3-dimethylaminopropyl)-N'-ethyl carbodiimide and N-hydroxysuccinimide) or additional components to be added (e.g., alginate, chitosan, fibrinogen, hyaluronan) to instigate crosslinking [123,127]. Berg et al. optimized a gelatin/alginate/Matrigel bioink to be used as a scaffold for human alveolar A549 cells [126]. When testing combinations using 1–10% (w/v) gelatin, it was reported that low amounts of gelation resulted in insufficient shape fidelity, but too high amounts resulted in unprintable hydrogels. A 2% (w/v) alginate and 3% (w/v) gelatin bioink was determined to be the best combination. When printing A549 cell-laden bioink, Matrigel was added to improve the bioink biocompatibility and expedite gelation.

Gelatin is often used in the form of gelatin-methacryloyl (GelMA), which is created through a gelatin and methacrylic anhydride reaction [122]. GelMA can be used for a broad range of tissue engineering applications, and is especially suitable for the production of load-bearing tissues like bone, cartilage, skin, and vascular networks [122]. A benefit of GelMA is that it does not require crosslinking agents or localized gelation during extrusion printing [122], but it does require the use of a photoinitiator followed by UV light exposure, which can cause decreased cell viability [128]. As well, high concentrations of GelMA (>7%) result in viability and biocompatibility deficits [129].

Liu et al. used a low concentration of GelMA (3%) and a cooling process to develop soft (~1.8 kPa) cell-laden constructs with high shape fidelity [129]. The GelMA bioink had self-healing (at concentrations of 3% and 4%) and shear-thinning properties. It was determined that higher GelMA concentrations and lower temperatures resulted in faster gelation speed, but lower concentrations resulted in more porous and flexible constructs [129]. In general, gelatin and its derivative, GelMA, are some of the most common natural bioinks used because of their thermo-sensitive capabilities and advantages this gives in altering viscosities.

2.10. Gellan Gum

Gellan gum is a linear, anionic polysaccharide secreted by the bacterium *Pseudomonas elodea* as a product of fermentation [130,131]. Gellan has a repeating pattern of one L-rhamnose, one D-glucuronic acid, and two D-glucose subunits [2,130]. It is biocompatible, biodegradable, and non-toxic with good mechanical properties and high gelling efficiency [2,130]. In the field of tissue engineering, gellan gum's primary applications are in bioprinting cartilage [3,4], skeletal tissue [132], and brain-like structures [133]. Although the main component of cartilage is collagen, gellan gum is added to collagen derivatives, such as GelMA, to improve the viscosity and increase the yield stress of the ink [4].

When gellan gum's biocompatibility is desired but stronger mechanical properties are necessary, gellan gum has successfully been added to a variety of other components. Hu et al. have shown that mixing gellan gum and PEGDA creates a bioink with good mechanical and rheological properties and high cell viability [2,3]. In one experiment, various structures were printed, using two automatic switching printheads (one filled with gellan gum and PEGDA, and one with poly(lactic acid) wire). After the structures were exposed to UV radiation to create scaffolds, their properties were tested. A rheometer tested the rheological properties, a universal testing machine was used for a compression test, a sodium hydroxide bath was used to test degradation, and the cell viability was assessed by live-dead staining [3]. After cross-linking, the bioink was able to withstand a shear rate of $> 300 \text{ s}^{-1}$, and formed a strong and stretchable structure with a high cell proliferation rate and cell viability above 90% during the culture time [3]. Chen et al. also found that combining gellan gum, sodium alginate, and a thixotropic magnesium phosphate-based gel to increase bioactivity produced a hybrid bioink with good gelation, mechanical, rheological, and printing properties that promoted cell proliferation and survival [5]. Cartilage test structures, such as human ears and noses, were printed, cross-linked in a calcium chloride solution, and tested using similar methods to those carried out

by Hu et al. [3,5]. All of the combination bioinks exhibited low viscosities and high shearing rates, [5], both of which improve printability. Additionally, the constructs with higher concentrations of gellan gum and lower concentrations of sodium alginate had better cell proliferation [5]. These two experiments illustrate gellan gum's ability to promote cell proliferation and improve the rheological properties of combination bioinks.

2.11. Hyaluronic Acid

Found in the ECM, HA naturally occurs in the ECM of mammalian tissues, including most organs and tissues of the central nervous system (CNS) [111,134–136]. HA is biocompatible, biodegradable, and bioresorbable, meaning it can be left in the body where it may dissolve or be absorbed [135]. It also has high porosity, which allows for easy diffusion of nutrients and waste products. HA has the ability to maintain a hydrated environment, making it an ideal tool for promoting wound healing [111,135]. The applications of HA extend from CNS and brain tissue engineering to bone and cartilage tissue engineering. It can be applied to organs and connective tissue and can be used as a space-filling scaffold [111,135–140]. HA lacks the mechanical integrity to function as an independent bioink; it has low stability caused by its high water solubility [111,141]. In addition, cells do not stick to the surface of HA, so it must be mixed with other components to promote cell adhesion [136]. The drawbacks of HA are often resolved by crosslinking and combining it with other components, as discussed in the following paragraphs, to form a hydrogel suitable for bioprinting [111,135,137,138,140,141].

Hou et al. developed a HA hydrogel modified with laminin, a component in the ECM that assists with cell adhesion and improves mechanical properties [139]. Laminin was immobilized on the backbone of the cross-linked HA and this hydrogel was implanted into cortical defects created in rats. After 6 and 12 weeks, the results showed that the hydrogel created a scaffold to foster infiltration, angiogenesis, and neurite extension while inhibiting glial scar formation. While this study did not test the hydrogel for bioprinting applications, it demonstrates a possible HA combination that exhibits advanced wound healing and mechanical properties.

Mazzocchi et al. hypothesized that methacrylated collagen I and thiolated HA could form a hydrogel with suitable properties for extrusion bioprinting [140]. A hydrogel composed of 3:1 collagen I: HA was ideal to bioprint a liver microenvironment due to the bioink's mechanical properties, printability, and high cellular viability. The liver model contained human hepatocytes and liver stellate cells; it was maintained for two weeks to demonstrate that the extrusion printing method did not adversely affect the cells. This study established a simple bioink that can be extrusion bioprinted and can be improved upon by the addition of ECM components like laminin or fibronectin. This bioink has the potential to provide a platform for the biofabrication of various types of tissue for human use.

2.12. Matrigel

Matrigel consists of a composite, gelatinous mixture extracted from mice tumors that mimics the human extracellular matrix (hECM) and contains proteins like laminin, collagen, and entactin [142–144]. This protein-based biomaterial provides a microenvironment for cells to grow in since it contains peptides and growth factors that help with cell growth and adhesion, components that are lacking from polysaccharide-based hydrogels [145]. Matrigel crosslinks at room temperature and, thus, needs a temperature-controlled system when using it for extrusion printing [144]. Matrigel has poor mechanical strength, like most protein-based hydrogels, so it is not ideal for printing [145].

Li et al. made a sodium alginate-Matrigel (SA-MA) hydrogel to print a 3D scaffold for assistance with the neural differentiation of ectomesenchymal stem cells in vitro and compared its properties to SA-hyaluronic acid and SA-gelatin hydrogels [146]. CaCl_2 was used as a crosslinking agent [146]. SA-MA and SA-gelatin had the shortest gelation time, and SA-MA was the most suitable combination for complete gelation. Viscosity was

altered by changing alginate and Matrigel concentrations, with 0.5/30 alginate/Matrigel concentration being the most suitable for printing and molding. The SA-MA hydrogel was the most suitable for cell growth and had the highest cell viability ($88.22 \pm 1.13\%$) of the hydrogels. Finally, increasing the Matrigel ratio of the bioink resulted in decreased scaffold degradability [146]. In another study, a collagen-Matrigel combination was used to print breast cancer cell-laden networks [143]. The addition of Matrigel allowed for the use of a lower collagen concentration (0.8 mg/mL) that more accurately represented collagen fiber networks used during cell culturing in previous studies. Matrigel can affect the morphology of the collagen fibers, as lower concentrations of Matrigel resulted in longer collagen fibers, although varying the Matrigel concentrations did not affect the collagen fiber alignment [143]. Although *in vivo* applications of Matrigel are limited due to its derivation from murine tumors, Matrigel bioinks present numerous opportunities for *ex vivo* research, including drug screening, 3D cell culturing, and cancer modelling applications [147,148].

2.13. Silk

Silk is found abundantly in nature, either from silkworms or spiders, and it has many diverse applications [149,150]. Silk fibroin (SF) is useful in tissue engineering due to its mechanical properties, biocompatibility, and controllable degradability [125,151,152]. This natural fibrous polymer has shear thinning properties that make it ideal for extrusion bioprinting [153]. SF is an attractive natural hydrogel component because it can accommodate chemical interactions other than covalent bonds, meaning it can be physically crosslinked, which removes the need for harsh crosslinking chemicals [125]. The disadvantages of SF include low viscosity and frequent clogging during printing [125].

Singh et al. developed a crosslinker-free hydrogel composed of silk and gelatin, where gelatin was used as a bulking agent [125]. These two components interacted by entanglement and physical crosslinking, eliminating the need for a crosslinking agent. A 3D bioprinted chondrocyte-laden construct of a human ear was printed and demonstrated good print fidelity of anatomical structures. The structure demonstrated *in vitro* and *in vivo* biocompatibility and provided promising advancements in cartilage tissue engineering. Rodriguez et al. aimed at producing a bioink to aid in soft tissue regeneration composed of SF, gelatin, and glycerol to induce physical crosslinking [153]. Irregular shapes, such as a human cheek segment, were printed and implanted in a mouse model. The study concluded that the system's rheology could be tuned by tuning the component ratios and concentrations to obtain different physical and mechanical properties. In addition, the biocompatible material maintained its shape for up to 3 months while promoting tissue integration.

3. Directions for Future Work and Conclusions

Future work in developing natural biomaterials for use in bioinks for tissue engineering aims to create more complex shapes, vasculature, and functional tissue structures. This can be achieved by optimizing the combination of biomaterials used for better mechanical, rheological, and biological properties. Optimizing and developing novel printing methods will also help to create larger and functioning organ structures. A proof of concept for this is FRESH, an innovative printing method used to print a human heart along with a functional tri-leaflet heart valve composed of collagen [82]. Additionally, improving the speed and resolution of printing is another goal of innovations in printing methods. For instance, Cellink and Prellis Biologics have introduced the Holograph X bioprinter, which utilizes holograms produced by spatial light modulators [154]. Using multiple printheads and materials to create complex structures can also be investigated. Future work involving adding drug-loaded microspheres to bioinks could increase cell viability along with stem cell differentiation and survival [116]. Incorporating drug laden microspheres into bioprinted constructs is one example of 4D bioprinting. 4D bioprinting is an extension of 3D bioprinting in which a fourth dimension—time—leads to a change in shape, functionality, or

biophysical characteristics of printed constructs due to internal or external stimuli [155,156]. Physical, chemical, or biological stimuli can be utilized in 4D bioprinting, including temperature changes, introduction of electric fields, pH changes, and enzymes [156]. Further investigating 4D bioprinting methods could lead to improved ability to produce structures that are difficult to obtain using traditional bioprinting methods, such as hollow tubes required for vasculature [157]. In addition, a co-culture construct was developed to imitate a brain and bioprinting was used to bioprint neurospheroid-laden designs [158]. This model could be expanded to explore the potential of using two or more multicomponent bioinks with or without the same crosslinker that can each support a different cell type. This would replicate a co-culture and allow the cells to thrive in a well-suited environment. Future work should investigate optimizing scaffold-free bioinks, which are composed only of cells without supporting biomaterials [30,31,33]. This should involve investigating methods of improving the structural integrity, reproducibility, and scalability of scaffold-free bioinks [35]. Transitioning towards bioinks consisting exclusively of cells could mitigate issues associated with scaffold-based bioinks, such as material toxicity, interruption of cell interactions, and impacts of scaffold degradation on mechanical properties [35]. Ultimately, scaffold-free bioinks could reduce immune responses in vivo and improve the biomimicry of bioprinted tissues [33,35]. Further challenges to be overcome include the scaling up of manufacturing bioink and its standardization.

Author Contributions: Writing—original draft preparation, C.B., J.C., R.L.K., N.Z.M., H.R., K.T.; writing—review and editing, C.B., J.C., R.L.K., N.Z.M., H.R., K.T., S.M.W.; supervision, S.M.W.; funding acquisition, S.M.W. All authors have read and agreed to the published version of the manuscript.

Funding: This work was supported by funding from the NSERC Discovery Grant program, the Michael Smith Foundation for Health Research and the Pacific Parkinson's Research Institute Innovation to Commercialization program, the Alzheimer's Association International Research Grant program and the Canada Research Chair program.

Institutional Review Board Statement: Not applicable.

Informed Consent Statement: The study did not report data or include humans or animals so statements have been excluded.

Data Availability Statement: Not applicable.

Conflicts of Interest: Willerth is the C.E.O. and co-founder of Axolotl Biosciences—a start-up that sells novel bioinks for bioprinting. The rest of the authors have no conflict to declare.

References

1. Cho, D.-W.; Kim, B.S.; Jang, J.; Gao, G.; Han, W.; Singh, N.K.; Cho, D.-W.; Kim, B.S.; Jang, J.; Gao, G.; et al. Conventional Bioinks. In *3D Bioprinting*; Springer International Publishing: Cham, Switzerland, 2019; pp. 31–40.
2. Wu, D.; Yu, Y.; Tan, J.; Huang, L.; Luo, B.; Lu, L.; Zhou, C. 3D bioprinting of gellan gum and poly (ethylene glycol) diacrylate based hydrogels to produce human-scale constructs with high-fidelity. *Mater. Des.* **2018**, *160*, 486–495. [[CrossRef](#)]
3. Hu, D.; Wu, D.; Huang, L.; Jiao, Y.; Li, L.; Lu, L.; Zhou, C. 3D bioprinting of cell-laden scaffolds for intervertebral disc regeneration. *Mater. Lett.* **2018**, *223*, 219–222. [[CrossRef](#)]
4. Mouser, V.H.M.; Levato, R.; Mensinga, A.; Dhert, W.J.A.; Gawlitta, D.; Malda, J. Bio-ink development for three-dimensional bioprinting of hetero-cellular cartilage constructs. *Connect. Tissue Res.* **2020**, *61*, 137–151. [[CrossRef](#)] [[PubMed](#)]
5. Chen, Y.; Xiong, X.; Liu, X.; Cui, R.; Wang, C.; Zhao, G.; Zhi, W.; Lu, M.; Duan, K.; Weng, J.; et al. 3D Bioprinting of shear-thinning hybrid bioinks with excellent bioactivity derived from gellan/alginate and thixotropic magnesium phosphate-based gels. *J. Mater. Chem. B* **2020**, *8*, 5500–5514. [[CrossRef](#)] [[PubMed](#)]
6. Frantz, C.; Stewart, K.M.; Weaver, V.M. The extracellular matrix at a glance. *J. Cell Sci.* **2010**, *123*, 4195–4200. [[CrossRef](#)]
7. Crapo, P.M.; Gilbert, T.W.; Badylak, S.F. An overview of tissue and whole organ decellularization processes. *Biomaterials* **2011**, *32*, 3233–3243. [[CrossRef](#)] [[PubMed](#)]
8. Paxton, N.; Smolan, W.; Böck, T.; Melchels, F.; Groll, J.; Jungst, T. Proposal to assess printability of bioinks for extrusion-based bioprinting and evaluation of rheological properties governing bioprintability. *Biofabrication* **2017**, *9*, 044107. [[CrossRef](#)]
9. Gillispie, G.; Prim, P.; Copus, J.; Fisher, J.; Mikos, A.G.; Yoo, J.J.; Atala, A.; Lee, S.J. Assessment methodologies for extrusion-based bioink printability. *Biofabrication* **2020**, *12*, 022003. [[CrossRef](#)]

10. Kryou, C.; Leva, V.; Chatzipetrou, M.; Zergioti, I. Bioprinting for liver transplantation. *Bioengineering* **2019**, *6*, 95. [[CrossRef](#)] [[PubMed](#)]
11. Li, J.; Chen, M.; Fan, X.; Zhou, H. Recent advances in bioprinting techniques: Approaches, applications and future prospects. *J. Transl. Med.* **2016**, *14*, 1–15. [[CrossRef](#)] [[PubMed](#)]
12. Kolesky, D.B.; Homan, K.A.; Skylar-Scott, M.A.; Lewis, J.A. Three-dimensional bioprinting of thick vascularized tissues. *Proc. Natl. Acad. Sci. USA* **2016**, *113*, 3179–3184. [[CrossRef](#)]
13. Donderwinkel, I.; Van Hest, J.C.M.; Cameron, N.R. Bio-inks for 3D bioprinting: Recent advances and future prospects. *Polym. Chem.* **2017**, *8*, 4451–4471. [[CrossRef](#)]
14. Demirtaş, T.T.; Irmak, G.; Gümüşderelioğlu, M. A bioprintable form of chitosan hydrogel for bone tissue engineering. *Biofabrication* **2017**, *9*, 035003. [[CrossRef](#)]
15. Guillemot, F.; Souquet, A.; Catros, S.; Guillotin, B. Laser-assisted cell printing: Principle, physical parameters versus cell fate and perspectives in tissue engineering. *Nanomedicine* **2010**, *5*, 507–515. [[CrossRef](#)] [[PubMed](#)]
16. Wang, Z.; Abdulla, R.; Parker, B.; Samanipour, R.; Ghosh, S.; Kim, K. A simple and high-resolution stereolithography-based 3D bioprinting system using visible light crosslinkable bioinks. *Biofabrication* **2015**, *7*, 045009. [[CrossRef](#)]
17. Panwar, A.; Tan, L.P. Current status of bioinks for micro-extrusion-based 3D bioprinting. *Molecules* **2016**, *21*, 685. [[CrossRef](#)]
18. Chimene, D.; Lennox, K.K.; Kaunas, R.R.; Gaharwar, A.K. Advanced Bioinks for 3D Printing: A Materials Science Perspective. *Ann. Biomed. Eng.* **2016**, *44*, 2090–2102. [[CrossRef](#)] [[PubMed](#)]
19. Baron, J.; Hazubski, S.; Otte, A. 3D Multi-Material Printing of an Anthropomorphic, Personalized Replacement Hand for Use in Neuroprosthetics Using 3D Scanning and Computer-Aided Design: First Proof-of-Technical-Concept Study. *Prosthesis* **2020**, *2*, 34. [[CrossRef](#)]
20. Aimar, A.; Palermo, A.; Innocenti, B. The Role of 3D Printing in Medical Applications: A State of the Art. *J. Healthc. Eng.* **2019**, *2019*, 1–10. [[CrossRef](#)]
21. Otte, A. 3D Computer-Aided Design Reconstructions and 3D Multi-Material Polymer Replica Printings of the First “Iron Hand” of Franconian Knight Gottfried (Götz) von Berlichingen (1480–1562): An Overview. *Prosthesis* **2020**, *2*, 27. [[CrossRef](#)]
22. Hölzl, K.; Lin, S.; Tytgat, L.; Van Vlierbergh, S.; Gu, L.; Ovsianikov, A. Bioink properties before, during and after 3D bioprinting. *Biofabrication* **2016**, *8*, 032002. [[CrossRef](#)] [[PubMed](#)]
23. Iram, D.; Riaz, R.; Iqbal, R.K. 3D Bioprinting: An attractive alternative to traditional organ transplantation. *Biomed. Sci. Eng.* **2019**, *5*, 007–018. [[CrossRef](#)]
24. Gopinathan, J.; Noh, I. Recent trends in bioinks for 3D printing. *Biomater. Res.* **2018**, *22*, 1–15. [[CrossRef](#)]
25. Williams, D.; Thayer, P.; Martinez, H.; Gatenholm, E.; Khademhosseini, A. A perspective on the physical, mechanical and biological specifications of bioinks and the development of functional tissues in 3D bioprinting. *Bioprinting* **2018**, *9*, 19–36. [[CrossRef](#)]
26. Malda, J.; Visser, J.; Melchels, F.P.; Jüngst, T.; Hennink, W.E.; Dhert, W.J.A.; Groll, J.; Hutmacher, D.W. 25th anniversary article: Engineering hydrogels for biofabrication. *Adv. Mater.* **2013**, *25*, 5011–5028. [[CrossRef](#)]
27. Bishop, E.S.; Mostafa, S.; Pakvasa, M.; Luu, H.H.; Lee, M.J.; Wolf, J.M.; Ameer, G.A.; He, T.C.; Reid, R.R. 3-D bioprinting technologies in tissue engineering and regenerative medicine: Current and future trends. *Genes Dis.* **2017**, *4*, 185–195. [[CrossRef](#)] [[PubMed](#)]
28. Parak, A.; Pradeep, P.; du Toit, L.C.; Kumar, P.; Choonara, Y.E.; Pillay, V. Functionalizing bioinks for 3D bioprinting applications. *Drug Discov. Today* **2019**, *24*, 198–205. [[CrossRef](#)]
29. Tsai, C.C.; Huang, R.N.; Sung, H.W.; Liang, H.C. In vitro evaluation of the genotoxicity of a naturally occurring crosslinking agent (genipin) for biologic tissue fixation. *J. Biomed. Mater. Res.* **2000**, *52*, 58–65. [[CrossRef](#)]
30. Hospodiuk, M.; Dey, M.; Sosnoski, D.; Ozbolat, I.T. The bioink: A comprehensive review on bioprintable materials. *Biotechnol. Adv.* **2017**, *35*, 217–239. [[CrossRef](#)]
31. Khoshnood, N.; Zamanian, A. A comprehensive review on scaffold-free bioinks for bioprinting. *Bioprinting* **2020**, *19*, e00088. [[CrossRef](#)]
32. Zafar, M.S.; Amin, F.; Fareed, M.A.; Ghabbani, H.; Riaz, S.; Khurshid, Z.; Kumar, N. Biomimetic aspects of restorative dentistry biomaterials. *Biomimetics* **2020**, *5*, 34. [[CrossRef](#)]
33. Norotte, C.; Marga, F.S.; Niklason, L.E.; Forgacs, G. Scaffold-free vascular tissue engineering using bioprinting. *Biomaterials* **2009**, *30*, 5910–5917. [[CrossRef](#)]
34. Ovsianikov, A.; Khademhosseini, A.; Mironov, V. The Synergy of Scaffold-Based and Scaffold-Free Tissue Engineering Strategies. *Trends Biotechnol.* **2018**, *36*, 348–357. [[CrossRef](#)]
35. Ozbolat, I.T. Scaffold-Based or Scaffold-Free Bioprinting: Competing or Complementing Approaches? *J. Nanotechnol. Eng. Med.* **2015**, *6*, 024701. [[CrossRef](#)]
36. Shimizu, T.; Yamato, M.; Kikuchi, A.; Okano, T. Cell sheet engineering for myocardial tissue reconstruction. *Biomaterials* **2003**, *24*, 2309–2316. [[CrossRef](#)]
37. Dahl, S.L.M.; Rhim, C.; Song, Y.C.; Niklason, L.E. Mechanical properties and compositions of tissue engineered and native arteries. *Ann. Biomed. Eng.* **2007**, *35*, 348–355. [[CrossRef](#)] [[PubMed](#)]
38. De la Vega, L.; Karmirian, K.; Willerth, S.M. Engineering Neural Tissue from Human Pluripotent Stem Cells Using Novel Small Molecule Releasing Microspheres. *Adv. Biosyst.* **2018**, *2*, 1800133. [[CrossRef](#)]

39. Wang, Z.; Lee, S.J.; Cheng, H.J.; Yoo, J.J.; Atala, A. 3D bioprinted functional and contractile cardiac tissue constructs. *Acta Biomater.* **2018**, *70*, 48–56. [[CrossRef](#)]
40. Jung, C.S.; Kim, B.K.; Lee, J.; Min, B.H.; Park, S.H. Development of Printable Natural Cartilage Matrix Bioink for 3D Printing of Irregular Tissue Shape. *Tissue Eng. Regen. Med.* **2018**, *15*, 155–162. [[CrossRef](#)]
41. Pourchet, L.J.; Thepot, A.; Albouy, M.; Courtial, E.J.; Boher, A.; Blum, L.J.; Marquette, C.A. Human Skin 3D Bioprinting Using Scaffold-Free Approach. *Adv. Healthc. Mater.* **2017**, *6*, 1601101. [[CrossRef](#)]
42. Lee, C.; Abelseh, E.; de la Vega, L.; Willerth, S.M. Bioprinting a novel glioblastoma tumor model using a fibrin-based bioink for drug screening. *Mater. Today Chem.* **2019**, *12*, 78–84. [[CrossRef](#)]
43. Cui, X.; Li, J.; Hartanto, Y.; Durham, M.; Tang, J.; Zhang, H.; Hooper, G.; Lim, K.; Woodfield, T. Advances in Extrusion 3D Bioprinting: A Focus on Multicomponent Hydrogel-Based Bioinks. *Adv. Healthc. Mater.* **2020**, *9*, 1901648. [[CrossRef](#)]
44. Gungor-Ozkerim, P.S.; Inci, I.; Zhang, Y.S.; Khademhosseini, A.; Dokmeci, M.R. Bioinks for 3D bioprinting: An overview. *Biomater. Sci.* **2018**, *6*, 915–946. [[CrossRef](#)] [[PubMed](#)]
45. Ashammakhi, N.; Ahadian, S.; Xu, C.; Montazerian, H.; Ko, H.; Nasiri, R.; Barros, N.; Khademhosseini, A. Bioinks and bioprinting technologies to make heterogeneous and biomimetic tissue constructs. *Mater. Today Bio* **2019**, *1*, 100008. [[CrossRef](#)] [[PubMed](#)]
46. Bertassoni, L.E.; Ceconi, M.; Manoharan, V.; Nikkhah, M.; Hjortnaes, J.; Cristino, A.L.; Barabaschi, G.; Demarchi, D.; Dokmeci, M.R.; Yang, Y.; et al. Hydrogel bioprinted microchannel networks for vascularization of tissue engineering constructs. *Lab Chip* **2014**, *14*, 2202–2211. [[CrossRef](#)] [[PubMed](#)]
47. Lee, K.; Cha, C. Advanced Polymer-Based Bioink Technology for Printing Soft Biomaterials. *Macromol. Res.* **2020**, *28*, 689–702. [[CrossRef](#)]
48. Zarrintaj, P.; Manouchehri, S.; Ahmadi, Z.; Saeb, M.R.; Urbanska, A.M.; Kaplan, D.L.; Mozafari, M. Agarose-based biomaterials for tissue engineering. *Carbohydr. Polym.* **2018**, *187*, 66–84. [[CrossRef](#)]
49. Aydin, L.; Kucuk, S.; Kenar, H. A universal self-eroding sacrificial bioink that enables bioprinting at room temperature. *Polym. Adv. Technol.* **2020**, *31*, 1634–1647. [[CrossRef](#)]
50. Gu, Q.; Tomaskovic-Crook, E.; Lozano, R.; Chen, Y.; Kapsa, R.M.; Zhou, Q.; Wallace, G.G.; Crook, J.M. Functional 3D Neural Mini-Tissues from Printed Gel-Based Bioink and Human Neural Stem Cells. *Adv. Healthc. Mater.* **2016**, *5*, 1429–1438. [[CrossRef](#)]
51. Yang, X.; Lu, Z.; Wu, H.; Li, W.; Zheng, L.; Zhao, J. Collagen-alginate as bioink for three-dimensional (3D) cell printing based cartilage tissue engineering. *Mater. Sci. Eng. C* **2018**, *83*, 195–201. [[CrossRef](#)]
52. Daly, A.C.; Critchley, S.E.; Rencsok, E.M.; Kelly, D.J. A comparison of different bioinks for 3D bioprinting of fibrocartilage and hyaline cartilage. *Biofabrication* **2016**, *8*, 045002. [[CrossRef](#)]
53. López-Marcial, G.R.; Zeng, A.Y.; Osuna, C.; Dennis, J.; García, J.M.; O’Connell, G.D. Agarose-Based Hydrogels as Suitable Bioprinting Materials for Tissue Engineering. *ACS Biomater. Sci. Eng.* **2018**, *4*, 3610–3616. [[CrossRef](#)]
54. Tan, Y.J.; Tan, X.; Yeong, W.Y.; Tor, S.B. Hybrid micro scaffold-based 3D bioprinting of multi-cellular constructs with high compressive strength: A new biofabrication strategy. *Sci. Rep.* **2016**, *6*, 39140. [[CrossRef](#)] [[PubMed](#)]
55. Forget, A.; Pique, R.-A.; Ahmadi, V.; Lüdeke, S.; Shastri, V.P. Mechanically Tailored Agarose Hydrogels through Molecular Alloying with β -Sheet Polysaccharides. *Macromol. Rapid Commun.* **2015**, *36*, 196–203. [[CrossRef](#)]
56. Gu, Y.; Schwarz, B.; Forget, A.; Barbero, A.; Martin, I.; Shastri, V.P. Advanced Bioink for 3D Bioprinting of Complex Free-Standing Structures with High Stiffness. *Bioengineering* **2020**, *7*, 141. [[CrossRef](#)] [[PubMed](#)]
57. Forget, A.; Blaeser, A.; Miessmer, F.; Köpf, M.; Campos, D.F.D.; Voelcker, N.H.; Blencowe, A.; Fischer, H.; Shastri, V.P. Mechanically Tunable Bioink for 3D Bioprinting of Human Cells. *Adv. Healthc. Mater.* **2017**, *6*, 1700255. [[CrossRef](#)] [[PubMed](#)]
58. Lee, K.Y.; Mooney, D.J. Alginate: Properties and biomedical applications. *Prog. Polym. Sci.* **2012**, *37*, 106–126. [[CrossRef](#)]
59. Emami, Z.; Ehsani, M.; Zandi, M.; Foudazi, R. Controlling alginate oxidation conditions for making alginate-gelatin hydrogels. *Carbohydr. Polym.* **2018**, *198*, 509–517. [[CrossRef](#)] [[PubMed](#)]
60. Bouhadir, K.H.; Lee, K.Y.; Alsberg, E.; Damm, K.L.; Anderson, K.W.; Mooney, D.J. Degradation of partially oxidized alginate and its potential application for tissue engineering. *Biotechnol. Prog.* **2001**, *17*, 945–950. [[CrossRef](#)] [[PubMed](#)]
61. Lee, J.; Hong, J.; Kim, W.; Kim, G.H. Bone-derived dECM/alginate bioink for fabricating a 3D cell-laden mesh structure for bone tissue engineering. *Carbohydr. Polym.* **2020**, *250*, 116914. [[CrossRef](#)] [[PubMed](#)]
62. Müller, M.; Öztürk, E.; Arlov, Ø.; Gatenholm, P.; Zenobi-Wong, M. Alginate Sulfate–Nanocellulose Bioinks for Cartilage Bioprinting Applications. *Ann. Biomed. Eng.* **2017**, *45*, 210–223. [[CrossRef](#)]
63. Jia, J.; Richards, D.J.; Pollard, S.; Tan, Y.; Rodriguez, J.; Visconti, R.P.; Trusk, T.C.; Yost, M.J.; Yao, H.; Markwald, R.R.; et al. Engineering alginate as bioink for bioprinting. *Acta Biomater.* **2014**, *10*, 4323–4331. [[CrossRef](#)]
64. Melo, B.A.G.; Jodat, Y.A.; Mehrotra, S.; Calabrese, M.A.; Kamperman, T.; Mandal, B.B.; Santana, M.H.A.; Alsberg, E.; Leijten, J.; Shin, S.R. 3D Printed Cartilage-Like Tissue Constructs with Spatially Controlled Mechanical Properties. *Adv. Funct. Mater.* **2019**, *29*, 1906330. [[CrossRef](#)]
65. Duan, B.; Hockaday, L.A.; Kang, K.H.; Butcher, J.T. 3D Bioprinting of heterogeneous aortic valve conduits with alginate/gelatin hydrogels. *J. Biomed. Mater. Res. Part A* **2013**, *101*, 1255–1264. [[CrossRef](#)]
66. Wang, Q.; Sun, J.; Yao, Q.; Ji, C.; Liu, J.; Zhu, Q. 3D printing with cellulose materials. *Cellulose* **2018**, *25*, 4275–4301. [[CrossRef](#)]
67. Nasatto, P.; Pignon, F.; Silveira, J.; Duarte, M.; Nosedá, M.; Rinaudo, M. Methylcellulose, a Cellulose Derivative with Original Physical Properties and Extended Applications. *Polymers* **2015**, *7*, 777–803. [[CrossRef](#)]

68. Janarthanan, G.; Tran, H.N.; Cha, E.; Lee, C.; Das, D.; Noh, I. 3D printable and injectable lactoferrin-loaded carboxymethyl cellulose-glycol chitosan hydrogels for tissue engineering applications. *Mater. Sci. Eng. C* **2020**, *113*, 111008. [[CrossRef](#)] [[PubMed](#)]
69. Sawkins, M.J.; Mistry, P.; Brown, B.N.; Shakesheff, K.M.; Bonassar, L.J.; Yang, J. Cell and protein compatible 3D bioprinting of mechanically strong constructs for bone repair. *Biofabrication* **2015**, *7*, 035004. [[CrossRef](#)]
70. Ninan, N.; Muthiah, M.; Park, I.K.; Elain, A.; Thomas, S.; Grohens, Y. Pectin/carboxymethyl cellulose/microfibrillated cellulose composite scaffolds for tissue engineering. *Carbohydr. Polym.* **2013**, *98*, 877–885. [[CrossRef](#)]
71. Wu, Y.; Lin, Z.Y.; Wenger, A.C.; Tam, K.C.; Tang, X. 3D bioprinting of liver-mimetic construct with alginate/cellulose nanocrystal hybrid bioink. *Bioprinting* **2018**, *9*, 1–6. [[CrossRef](#)]
72. Jiang, Y.; Zhou, J.; Shi, H.; Zhao, G.; Zhang, Q.; Feng, C.; Xu, X. Preparation of cellulose nanocrystal/oxidized dextran/gelatin (CNC/OD/GEL) hydrogels and fabrication of a CNC/OD/GEL scaffold by 3D printing. *J. Mater. Sci.* **2020**, *55*, 2618–2635. [[CrossRef](#)]
73. Markstedt, K.; Mantas, A.; Tournier, I.; Martínez Ávila, H.; Hägg, D.; Gatenholm, P. 3D bioprinting human chondrocytes with nanocellulose-alginate bioink for cartilage tissue engineering applications. *Biomacromolecules* **2015**, *16*, 1489–1496. [[CrossRef](#)] [[PubMed](#)]
74. Rees, A.; Powell, L.C.; Chinga-Carrasco, G.; Gethin, D.T.; Syverud, K.; Hill, K.E.; Thomas, D.W. 3D bioprinting of carboxymethylated-periodate oxidized nanocellulose constructs for wound dressing applications. *Biomed Res. Int.* **2015**, *2015*, 1–7. [[CrossRef](#)] [[PubMed](#)]
75. He, Y.; Derakhshanfar, S.; Zhong, W.; Li, B.; Lu, F.; Xing, M.; Li, X. Characterization and Application of Carboxymethyl Chitosan-Based Bioink in Cartilage Tissue Engineering. *J. Nanomater.* **2020**, *2020*, 1–11. [[CrossRef](#)]
76. Wu, Q.; Therriault, D.; Heuzey, M.C. Processing and Properties of Chitosan Inks for 3D Printing of Hydrogel Microstructures. *ACS Biomater. Sci. Eng.* **2018**, *4*, 2643–2652. [[CrossRef](#)]
77. Ricard-Blum, S. The Collagen Family. *Cold Spring Harb. Perspect. Biol.* **2011**, *3*, a004978. [[CrossRef](#)]
78. Shoulders, M.D.; Raines, R.T. Collagen Structure and Stability. *Annu. Rev. Biochem.* **2009**, *78*, 929–958. [[CrossRef](#)] [[PubMed](#)]
79. Lynn, A.K.; Yannas, I.V.; Bonfield, W. Antigenicity and immunogenicity of collagen. *J. Biomed. Mater. Res. Part B Appl. Biomater.* **2004**, *71*, 343–354. [[CrossRef](#)]
80. Kumar, V.A.; Taylor, N.L.; Jalan, A.A.; Hwang, L.K.; Wang, B.K.; Hartgerink, J.D. A nanostructured synthetic collagen mimic for hemostasis. *Biomacromolecules* **2014**, *15*, 1484–1490. [[CrossRef](#)]
81. Lee, H.; Cho, D.W. One-step fabrication of an organ-on-a-chip with spatial heterogeneity using a 3D bioprinting technology. *Lab Chip* **2016**, *16*, 2618–2625. [[CrossRef](#)]
82. Lee, A.; Hudson, A.R.; Shiwarski, D.J.; Tashman, J.W.; Hinton, T.J.; Yerneni, S.; Bliley, J.M.; Campbell, P.G.; Feinberg, A.W. 3D bioprinting of collagen to rebuild components of the human heart. *Science* **2019**, *365*, 482–487. [[CrossRef](#)] [[PubMed](#)]
83. Lee, W.; Lee, V.; Polio, S.; Keegan, P.; Lee, J.-H.; Fischer, K.; Park, J.-K.; Yoo, S.-S. On-demand three-dimensional freeform fabrication of multi-layered hydrogel scaffold with fluidic channels. *Biotechnol. Bioeng.* **2010**, *105*, 1178–1186. [[CrossRef](#)] [[PubMed](#)]
84. Diamantides, N.; Wang, L.; Pruiksma, T.; Siemiatkoski, J.; Dugopolski, C.; Shortkroff, S.; Kennedy, S.; Bonassar, L.J. Correlating rheological properties and printability of collagen bioinks: The effects of riboflavin photocrosslinking and pH. *Biofabrication* **2017**, *9*, 034102. [[CrossRef](#)] [[PubMed](#)]
85. Rhee, S.; Puetzer, J.L.; Mason, B.N.; Reinhart-King, C.A.; Bonassar, L.J. 3D Bioprinting of Spatially Heterogeneous Collagen Constructs for Cartilage Tissue Engineering. *ACS Biomater. Sci. Eng.* **2016**, *2*, 1800–1805. [[CrossRef](#)] [[PubMed](#)]
86. Osidak, E.O.; Karalkin, P.A.; Osidak, M.S.; Parfenov, V.A.; Sivogrivov, D.E.; Pereira, F.D.A.S.; Gryadunova, A.A.; Koudan, E.V.; Khesuani, Y.D.; Kasyanov, V.A.; et al. Viscoll collagen solution as a novel bioink for direct 3D bioprinting. *J. Mater. Sci. Mater. Med.* **2019**, *30*, 1–12. [[CrossRef](#)]
87. Diamantides, N.; Dugopolski, C.; Blahut, E.; Kennedy, S.; Bonassar, L.J. High density cell seeding affects the rheology and printability of collagen bioinks. *Biofabrication* **2019**, *11*, 045016. [[CrossRef](#)]
88. Liu, S.; Huang, D.; Hu, Y.; Zhang, J.; Chen, B.; Zhang, H.; Dong, X.; Tong, R.; Li, Y.; Zhou, W. Sodium alginate/collagen composite multiscale porous scaffolds containing poly(ϵ -caprolactone) microspheres fabricated based on additive manufacturing technology. *RSC Adv.* **2020**, *10*, 39241–39250. [[CrossRef](#)]
89. Heidenreich, A.C.; Pérez-Recalde, M.; González Wusener, A.; Hermida, É.B. Collagen and chitosan blends for 3D bioprinting: A rheological and printability approach. *Polym. Test.* **2020**, *82*, 106297. [[CrossRef](#)]
90. Keane, T.J.; Swinehart, I.T.; Badylak, S.F. Methods of tissue decellularization used for preparation of biologic scaffolds and in vivo relevance. *Methods* **2015**, *84*, 25–34. [[CrossRef](#)]
91. Pati, F.; Jang, J.; Ha, D.H.; Won Kim, S.; Rhie, J.W.; Shim, J.H.; Kim, D.H.; Cho, D.W. Printing three-dimensional tissue analogues with decellularized extracellular matrix bioink. *Nat. Commun.* **2014**, *5*, 3935. [[CrossRef](#)] [[PubMed](#)]
92. Han, W.; Singh, N.K.; Kim, J.J.; Kim, H.; Kim, B.S.; Park, J.Y.; Jang, J.; Cho, D.W. Directed differential behaviors of multipotent adult stem cells from decellularized tissue/organ extracellular matrix bioinks. *Biomaterials* **2019**, *224*, 119496. [[CrossRef](#)] [[PubMed](#)]
93. Das, S.; Kim, S.W.; Choi, Y.J.; Lee, S.; Lee, S.H.; Kong, J.S.; Park, H.J.; Cho, D.W.; Jang, J. Decellularized extracellular matrix bioinks and the external stimuli to enhance cardiac tissue development in vitro. *Acta Biomater.* **2019**, *95*, 188–200. [[CrossRef](#)]
94. Shin, Y.J.; Shafraanek, R.T.; Tsui, J.H.; Walcott, J.; Nelson, A.; Kim, D.H. 3D bioprinting of mechanically tuned bioinks derived from cardiac decellularized extracellular matrix. *Acta Biomater.* **2020**, *119*, 75–88. [[CrossRef](#)]

95. Jang, J.; Kim, T.G.; Kim, B.S.; Kim, S.W.; Kwon, S.M.; Cho, D.W. Tailoring mechanical properties of decellularized extracellular matrix bioink by vitamin B2-induced photo-crosslinking. *Acta Biomater.* **2016**, *33*, 88–95. [[CrossRef](#)]
96. Jang, J.; Park, H.J.; Kim, S.W.; Kim, H.; Park, J.Y.; Na, S.J.; Kim, H.J.; Park, M.N.; Choi, S.H.; Park, S.H.; et al. 3D printed complex tissue construct using stem cell-laden decellularized extracellular matrix bioinks for cardiac repair. *Biomaterials* **2017**, *112*, 264–274. [[CrossRef](#)] [[PubMed](#)]
97. Kim, B.S.; Kwon, Y.W.; Kong, J.S.; Park, G.T.; Gao, G.; Han, W.; Kim, M.B.; Lee, H.; Kim, J.H.; Cho, D.W. 3D cell printing of in vitro stabilized skin model and in vivo pre-vascularized skin patch using tissue-specific extracellular matrix bioink: A step towards advanced skin tissue engineering. *Biomaterials* **2018**, *168*, 38–53. [[CrossRef](#)]
98. Jorgensen, A.M.; Chou, Z.; Gillispie, G.; Lee, S.J.; Yoo, J.J.; Soker, S.; Atala, A. Decellularized skin extracellular matrix (dsECM) improves the physical and biological properties of fibrinogen hydrogel for skin bioprinting applications. *Nanomaterials* **2020**, *10*, 1484. [[CrossRef](#)]
99. Ahn, G.; Min, K.H.; Kim, C.; Lee, J.S.; Kang, D.; Won, J.Y.; Cho, D.W.; Kim, J.Y.; Jin, S.; Yun, W.S.; et al. Precise stacking of decellularized extracellular matrix based 3D cell-laden constructs by a 3D cell printing system equipped with heating modules. *Sci. Rep.* **2017**, *7*, 8624. [[CrossRef](#)] [[PubMed](#)]
100. Lee, H.; Han, W.; Kim, H.; Ha, D.H.; Jang, J.; Kim, B.S.; Cho, D.W. Development of Liver Decellularized Extracellular Matrix Bioink for Three-Dimensional Cell Printing-Based Liver Tissue Engineering. *Biomacromolecules* **2017**, *18*, 1229–1237. [[CrossRef](#)] [[PubMed](#)]
101. Shi, L.; Hu, Y.; Ullah, M.W.; Ullah, I.; Ou, H.; Zhang, W.; Xiong, L.; Zhang, X. Cryogenic free-form extrusion bioprinting of decellularized small intestinal submucosa for potential applications in skin tissue engineering. *Biofabrication* **2019**, *11*, 035023. [[CrossRef](#)]
102. Kim, H.; Jang, J.; Park, J.; Lee, K.P.; Lee, S.; Lee, D.M.; Kim, K.H.; Kim, H.K.; Cho, D.W. Shear-induced alignment of collagen fibrils using 3D cell printing for corneal stroma tissue engineering. *Biofabrication* **2019**, *11*, 035017. [[CrossRef](#)] [[PubMed](#)]
103. Kim, J.-Y.; Ahn, G.; Kim, C.; Lee, J.-S.; Lee, I.-G.; An, S.-H.; Yun, W.-S.; Kim, S.-Y.; Shim, J.-H. Synergistic Effects of Beta Tri-Calcium Phosphate and Porcine-Derived Decellularized Bone Extracellular Matrix in 3D-Printed Polycaprolactone Scaffold on Bone Regeneration. *Macromol. Biosci.* **2018**, *18*, 1800025. [[CrossRef](#)] [[PubMed](#)]
104. Toprakhisar, B.; Nadernezhad, A.; Bakirci, E.; Khani, N.; Skvortsov, G.A.; Koc, B. Development of Bioink from Decellularized Tendon Extracellular Matrix for 3D Bioprinting. *Macromol. Biosci.* **2018**, *18*, e1800024. [[CrossRef](#)] [[PubMed](#)]
105. Zhao, F.; Cheng, J.; Sun, M.; Yu, H.; Wu, N.; Li, Z.; Zhang, J.; Li, Q.; Yang, P.; Liu, Q.; et al. Digestion degree is a key factor to regulate the printability of pure tendon decellularized extracellular matrix bio-ink in extrusion-based 3D cell printing. *Biofabrication* **2020**, *12*, 045011. [[CrossRef](#)]
106. Sun, G.; Mao, J.J. Engineering dextran-based scaffolds for drug delivery and tissue repair. *Nanomedicine* **2012**, *7*, 1771–1784. [[CrossRef](#)]
107. Turner, P.R.; Murray, E.; McAdam, C.J.; McConnell, M.A.; Cabral, J.D. Peptide Chitosan/Dextran Core/Shell Vascularized 3D Constructs for Wound Healing. *ACS Appl. Mater. Interfaces* **2020**, *12*, 32328–32339. [[CrossRef](#)]
108. Du, Z.; Li, N.; Hua, Y.; Shi, Y.; Bao, C.; Zhang, H.; Yang, Y.; Lin, Q.; Zhu, L. Physiological pH-dependent gelation for 3D printing based on the phase separation of gelatin and oxidized dextran. *Chem. Commun.* **2017**, *53*, 13023–13026. [[CrossRef](#)]
109. Geng, X.; Yuan, L.; Mo, X. Oxidized dextran/amino gelatin/hyaluronic acid semi-interpenetrating network hydrogels for tissue engineering application. *Adv. Mat. Res.* **2013**, *627*, 745–750. [[CrossRef](#)]
110. Inci, I.; Kirsebom, H.; Galaev, I.Y.; Mattiasson, B.; Piskin, E. Gelatin cryogels crosslinked with oxidized dextran and containing freshly formed hydroxyapatite as potential bone tissue-engineering scaffolds. *J. Tissue Eng. Regen. Med.* **2013**, *7*, 584–588. [[CrossRef](#)]
111. Pescosolido, L.; Schuurman, W.; Malda, J.; Matricardi, P.; Alhaique, F.; Coviello, T.; Van Weeren, P.R.; Dhert, W.J.A.; Hennink, W.E.; Vermonden, T. Hyaluronic acid and dextran-based semi-IPN hydrogels as biomaterials for bioprinting. *Biomacromolecules* **2011**, *12*, 1831–1838. [[CrossRef](#)]
112. Harman, D.G.; Gorkin, R.; Stevens, L.; Thompson, B.; Wagner, K.; Weng, B.; Chung, J.H.Y.; Panhuis, M.I.H.; Wallace, G.G. Poly(3,4-ethylenedioxythiophene):dextran sulfate (PEDOT:DS)-A highly processable conductive organic biopolymer. *Acta Biomater.* **2015**, *14*, 33–42. [[CrossRef](#)] [[PubMed](#)]
113. de Melo, B.A.G.; Jodat, Y.A.; Cruz, E.M.; Benincasa, J.C.; Shin, S.R.; Porcionatto, M.A. Strategies to use fibrinogen as bioink for 3D bioprinting fibrin-based soft and hard tissues. *Acta Biomater.* **2020**, *117*, 60–76. [[CrossRef](#)] [[PubMed](#)]
114. Abelseth, E.; Abelseth, L.; De La Vega, L.; Beyer, S.T.; Wadsworth, S.J.; Willerth, S.M. 3D Printing of Neural Tissues Derived from Human Induced Pluripotent Stem Cells Using a Fibrin-Based Bioink. *ACS Biomater. Sci. Eng.* **2019**, *5*, 234–243. [[CrossRef](#)]
115. De La Vega, L.; Rosas Gómez, D.A.; Abelseth, E.; Abelseth, L.; Allisson Da Silva, V.; Willerth, S.M. 3D Bioprinting Human Induced Pluripotent Stem Cell-Derived Neural Tissues Using a Novel Lab-on-a-Printer Technology. *Appl. Sci.* **2018**, *8*, 2414. [[CrossRef](#)]
116. Sharma, R.; Smits, I.P.M.; De La Vega, L.; Lee, C.; Willerth, S.M. 3D Bioprinting Pluripotent Stem Cell Derived Neural Tissues Using a Novel Fibrin Bioink Containing Drug Releasing Microspheres. *Front. Bioeng. Biotechnol.* **2020**, *8*, 57. [[CrossRef](#)]
117. Weisel, J.W. The mechanical properties of fibrin for basic scientists and clinicians. *Biophys. Chem.* **2004**, *112*, 267–276. [[CrossRef](#)]
118. Smits, I.P.M.; Blaschuk, O.W.; Willerth, S.M. Novel N-cadherin antagonist causes glioblastoma cell death in a 3D bioprinted co-culture model. *Biochem. Biophys. Res. Commun.* **2020**, *529*, 162–168. [[CrossRef](#)] [[PubMed](#)]

119. Dai, X.; Liu, L.; Ouyang, J.; Li, X.; Zhang, X.; Lan, Q.; Xu, T. Coaxial 3D bioprinting of self-assembled multicellular heterogeneous tumor fibers. *Sci. Rep.* **2017**, *7*, 1–11. [[CrossRef](#)]
120. Hinton, T.J.; Jallerat, Q.; Palchesko, R.N.; Park, J.H.; Grodzicki, M.S.; Shue, H.J.; Ramadan, M.H.; Hudson, A.R.; Feinberg, A.W. Three-dimensional printing of complex biological structures by freeform reversible embedding of suspended hydrogels. *Sci. Adv.* **2015**, *1*, e1500758. [[CrossRef](#)]
121. Anil Kumar, S.; Alonzo, M.; Allen, S.C.; Abelseh, L.; Thakur, V.; Akimoto, J.; Ito, Y.; Willerth, S.M.; Suggs, L.; Chattopadhyay, M.; et al. A Visible Light-Cross-Linkable, Fibrin-Gelatin-Based Bioprinted Construct with Human Cardiomyocytes and Fibroblasts. *ACS Biomater. Sci. Eng.* **2019**, *5*, 4551–4563. [[CrossRef](#)]
122. Sun, M.; Sun, X.; Wang, Z.; Guo, S.; Yu, G.; Yang, H. Synthesis and properties of gelatin methacryloyl (GelMA) hydrogels and their recent applications in load-bearing tissue. *Polymers* **2018**, *10*, 1290. [[CrossRef](#)]
123. Wang, X.; Ao, Q.; Tian, X.; Fan, J.; Tong, H.; Hou, W.; Bai, S. Gelatin-based hydrogels for organ 3D bioprinting. *Polymers* **2017**, *9*, 401. [[CrossRef](#)] [[PubMed](#)]
124. Van Den Bulcke, A.I.; Bogdanov, B.; De Rooze, N.; Schacht, E.H.; Cornelissen, M.; Berghmans, H. Structural and rheological properties of methacrylamide modified gelatin hydrogels. *Biomacromolecules* **2000**, *1*, 31–38. [[CrossRef](#)]
125. Singh, Y.P.; Bandyopadhyay, A.; Mandal, B.B. 3D Bioprinting Using Cross-Linker-Free Silk-Gelatin Bioink for Cartilage Tissue Engineering. *ACS Appl. Mater. Interfaces* **2019**, *11*, 33684–33696. [[CrossRef](#)]
126. Berg, J.; Hiller, T.; Kissner, M.S.; Qazi, T.H.; Duda, G.N.; Hocke, A.C.; Hippenstiel, S.; Elomaa, L.; Weinhart, M.; Fahrenson, C.; et al. Optimization of cell-laden bioinks for 3D bioprinting and efficient infection with influenza A virus. *Sci. Rep.* **2018**, *8*, 13877. [[CrossRef](#)]
127. Kuijpers, A.J.; Engbers, G.H.M.; Krijgsveld, J.; Zaat, S.A.J.; Dankert, J.; Feijen, J. Cross-linking and characterisation of gelatin matrices for biomedical applications. *J. Biomater. Sci. Polym. Ed.* **2000**, *11*, 225–243. [[CrossRef](#)] [[PubMed](#)]
128. Xu, H.; Casillas, J.; Krishnamoorthy, S.; Xu, C. Effects of Irgacure 2959 and lithium phenyl-2,4,6-trimethylbenzoylphosphinate on cell viability, physical properties, and microstructure in 3D bioprinting of vascular-like constructs. *Biomed. Mater.* **2020**, *15*, 055021. [[CrossRef](#)]
129. Liu, W.; Heinrich, M.A.; Zhou, Y.; Akpek, A.; Hu, N.; Liu, X.; Guan, X.; Zhong, Z.; Jin, X.; Khademhosseini, A.; et al. Extrusion Bioprinting of Shear-Thinning Gelatin Methacryloyl Bioinks. *Adv. Healthc. Mater.* **2017**, *6*, 1601451. [[CrossRef](#)]
130. Zia, K.M.; Tabasum, S.; Khan, M.F.; Akram, N.; Akhter, N.; Noreen, A.; Zuber, M. Recent trends on gellan gum blends with natural and synthetic polymers: A review. *Int. J. Biol. Macromol.* **2018**, *109*, 1068–1087. [[CrossRef](#)]
131. Nussinovitch, A. Gellan gum. *Hydrocolloid Appl.* **1997**, 63–82. [[CrossRef](#)]
132. Cidonio, G.; Cooke, M.; Glinka, M.; Dawson, J.I.; Grover, L.; Oreffo, R.O.C. Printing bone in a gel: Using nanocomposite bioink to print functionalised bone scaffolds. *Mater. Today Bio* **2019**, *4*, 100028. [[CrossRef](#)] [[PubMed](#)]
133. Lozano, R.; Stevens, L.; Thompson, B.C.; Gilmore, K.J.; Gorkin III, R.; Stewart, E.M.; Panhuis, M.I.H.; Romero-Ortega, M.; Wallace, G.G. 3D printing of layered brain-like structures using peptide modified gellan gum substrates. *Biomaterials* **2015**, *67*, 264–273. [[CrossRef](#)] [[PubMed](#)]
134. Park, S.H.; Seo, J.Y.; Park, J.Y.; Ji, Y.B.; Kim, K.; Choi, H.S.; Choi, S.; Kim, J.H.; Min, B.H.; Kim, M.S. An injectable, click-crosslinked, cytomodulin-modified hyaluronic acid hydrogel for cartilage tissue engineering. *NPG Asia Mater.* **2019**, *11*, 30. [[CrossRef](#)]
135. Collins, M.N.; Birkinshaw, C. Hyaluronic acid based scaffolds for tissue engineering—A review. *Carbohydr. Polym.* **2013**, *92*, 1262–1279. [[CrossRef](#)]
136. Wang, X.; He, J.; Wang, Y.; Cui, F.Z. Hyaluronic acid-based scaffold for central neural tissue engineering. *Interface Focus* **2012**, *2*, 278–291. [[CrossRef](#)] [[PubMed](#)]
137. Hou, S.; Xu, Q.; Tian, W.; Cui, F.; Cai, Q.; Ma, J.; Lee, I.S. The repair of brain lesion by implantation of hyaluronic acid hydrogels modified with laminin. *J. Neurosci. Methods* **2005**, *148*, 60–70. [[CrossRef](#)] [[PubMed](#)]
138. Wang, T.W.; Spector, M. Development of hyaluronic acid-based scaffolds for brain tissue engineering. *Acta Biomater.* **2009**, *5*, 2371–2384. [[CrossRef](#)]
139. Lin, C.M.; Lin, J.W.; Chen, Y.C.; Shen, H.H.; Wei, L.; Yeh, Y.S.; Chiang, Y.H.; Shih, R.; Chiu, P.L.; Hung, K.S.; et al. Hyaluronic acid inhibits the glial scar formation after brain damage with tissue loss in rats. *Surg. Neurol.* **2009**, *72*, S50–S54. [[CrossRef](#)]
140. Mazzocchi, A.; Devarasetty, M.; Huntwork, R.; Soker, S.; Skardal, A. Optimization of collagen type I-hyaluronan hybrid bioink for 3D bioprinted liver microenvironments. *Biofabrication* **2019**, *11*, 015003. [[CrossRef](#)] [[PubMed](#)]
141. Collins, M.N.; Birkinshaw, C. Comparison of the effectiveness of four different crosslinking agents with hyaluronic acid hydrogel films for tissue-culture applications. *J. Appl. Polym. Sci.* **2007**, *104*, 3183–3191. [[CrossRef](#)]
142. Hiller, T.; Berg, J.; Elomaa, L.; Röhrs, V.; Ullah, I.; Schaar, K.; Dietrich, A.C.; Al-Zeer, M.A.; Kurtz, A.; Hocke, A.C.; et al. Generation of a 3D liver model comprising human extracellular matrix in an alginate/gelatin-based bioink by extrusion bioprinting for infection and transduction studies. *Int. J. Mol. Sci.* **2018**, *19*, 3129. [[CrossRef](#)]
143. Nerger, B.A.; Brun, P.T.; Nelson, C.M. Microextrusion printing cell-laden networks of type I collagen with patterned fiber alignment and geometry. *Soft Matter* **2019**, *15*, 5728–5738. [[CrossRef](#)] [[PubMed](#)]
144. Snyder, J.E.; Hamid, Q.; Wang, C.; Chang, R.; Emami, K.; Wu, H.; Sun, W. Bioprinting cell-laden matrigel for radioprotection study of liver by pro-drug conversion in a dual-tissue microfluidic chip. *Biofabrication* **2011**, *3*, 034122. [[CrossRef](#)]
145. Fan, R.; Piou, M.; Darling, E.; Cormier, D.; Sun, J.; Wan, J. Bio-printing cell-laden Matrigel-agarose constructs. *J. Biomater. Appl.* **2016**, *31*, 684–692. [[CrossRef](#)]

146. Li, Y.; Cao, X.; Deng, W.; Yu, Q.; Sun, C.; Ma, P.; Shao, F.; Yusif, M.M.; Ge, Z.; Wang, K.; et al. 3D printable Sodium alginate-Matrigel (SA-MA) hydrogel facilitated ectomesenchymal stem cells (EMSCs) neuron differentiation. *J. Biomater. Appl.* **2020**, *35*, 709–719. [[CrossRef](#)]
147. Benton, G.; Arnaoutova, I.; George, J.; Kleinman, H.K.; Koblinski, J. Matrigel: From discovery and ECM mimicry to assays and models for cancer research. *Adv. Drug Deliv. Rev.* **2014**, *79*, 3–18. [[CrossRef](#)]
148. Benton, G.; Kleinman, H.K.; George, J.; Arnaoutova, I. Multiple uses of basement membrane-like matrix (BME/Matrigel) in vitro and in vivo with cancer cells. *Int. J. Cancer* **2011**, *128*, 1751–1757. [[CrossRef](#)]
149. Kundu, B.; Kurland, N.E.; Bano, S.; Patra, C.; Engel, F.B.; Yadavalli, V.K.; Kundu, S.C. Silk proteins for biomedical applications: Bioengineering perspectives. *Prog. Polym. Sci.* **2014**, *39*, 251–267. [[CrossRef](#)]
150. Vepari, C.; Kaplan, D.L. Silk as a biomaterial. *Prog. Polym. Sci.* **2007**, *32*, 991–1007. [[CrossRef](#)]
151. Singh, Y.P.; Moses, J.C.; Bhunia, B.K.; Nandi, S.K.; Mandal, B.B. Hierarchically structured seamless silk scaffolds for osteochondral interface tissue engineering. *J. Mater. Chem. B* **2018**, *6*, 5671–5688. [[CrossRef](#)] [[PubMed](#)]
152. Das, S.; Pati, F.; Choi, Y.J.; Rijal, G.; Shim, J.H.; Kim, S.W.; Ray, A.R.; Cho, D.W.; Ghosh, S. Bioprintable, cell-laden silk fibroin-gelatin hydrogel supporting multilineage differentiation of stem cells for fabrication of three-dimensional tissue constructs. *Acta Biomater.* **2015**, *11*, 233–246. [[CrossRef](#)]
153. Rodriguez, M.J.; Brown, J.; Giordano, J.; Lin, S.J.; Omenetto, F.G.; Kaplan, D.L. Silk based bioinks for soft tissue reconstruction using 3-dimensional (3D) printing with in vitro and in vivo assessments. *Biomaterials* **2017**, *117*, 105–115. [[CrossRef](#)]
154. Lee, M.; Rizzo, R.; Surman, F.; Zenobi-Wong, M. Guiding Lights: Tissue Bioprinting Using Photoactivated Materials. *Chem. Rev.* **2020**, *120*, 10950–11027. [[CrossRef](#)]
155. Miri, A.K.; Khalilpour, A.; Cecen, B.; Maharjan, S.; Shin, S.R.; Khademhosseini, A. Multiscale bioprinting of vascularized models. *Biomaterials* **2019**, *198*, 204–216. [[CrossRef](#)] [[PubMed](#)]
156. Yang, Q.; Gao, B.; Xu, F. Recent Advances in 4D Bioprinting. *Biotechnol. J.* **2020**, *15*, e1900086. [[CrossRef](#)] [[PubMed](#)]
157. Kirillova, A.; Maxson, R.; Stoychev, G.; Gomillion, C.T.; Ionov, L. 4D Biofabrication Using Shape-Morphing Hydrogels. *Adv. Mater.* **2017**, *29*, 1703443. [[CrossRef](#)] [[PubMed](#)]
158. Li, Y.C.E.; Jodat, Y.A.; Samanipour, R.; Zorzi, G.; Zhu, K.; Hirano, M.; Chang, K.; Arnaout, A.; Hassan, S.; Matharu, N.; et al. Toward a neurospheroid niche model: Optimizing embedded 3D bioprinting for fabrication of neurospheroid brain-like co-culture constructs. *Biofabrication* **2020**, *13*, 015014. [[CrossRef](#)] [[PubMed](#)]